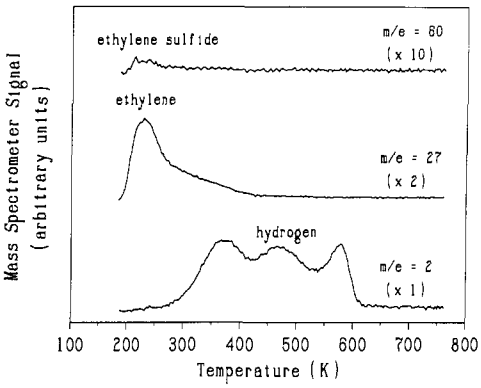

Figure 2. Temperature-programmed reaction of ethylene sulfide on Mo(110). Adsorption occurred at 140 K, and the heating rate was approximately 15 K/s. The multiplication factors are referenced to hydrogen and are uncorrected for degree of fragmentation and ionization efficiency in the mass spectrometer. The intensity of the ethylene sulfide peak is so low that ethylene sulfide cracking at $m/e = 27$ does not contribute to the ethylene peak.

olution of gaseous ethylene. In Figure 1 are shown the partial pressures of ethylene and ethylene sulfide (measured mass spectrometrically) in the ultrahigh vacuum chamber as a function of time during the ethylene sulfide dose for a crystal temperature of 140 K. The ethylene pressure rises immediately upon exposure of the surface to ethylene sulfide. Ethylene production reaches a maximum rate at an exposure of approximately 10 s. After 20 s, the rate of formation drops. Ethylene production stops after 60 s. Production of ethylene upon adsorption was evident for crystal temperatures as low as 100 K, the lowest temperature we could access. The ethylene yield was not dependent upon crystal temperature between 100 and 140 K, as measured by the ethylene pressure curves and by the sulfur Auger spectra after reaction. Ethylene sulfide and ethylene are the only species whose pressure was observed to change. Notably, no formation of ethane or displacement of water, dihydrogen, or carbon monoxide from the crystal or the chamber walls could be detected.

Temperature-programmed reaction after ethylene sulfide adsorption demonstrates that not all ethylene sulfide reacts to form gas-phase ethylene upon adsorption. Three products are detected at saturation exposures (60 s) during temperature-programmed reaction, as shown in Figure 2: ethylene at 220 K, small amounts of ethylene sulfide at 220 K, and dihydrogen at 375, 460, and 575 K. The nature of the ethylene peak is under investigation, principally by X-ray photoemission spectroscopy. The dihydrogen peaks at 375 and 460 K likely result from a combination of desorption and limited states, as discussed previously.[1a,b] The dihydrogen peak at 575 K is assigned to the decomposition of a surface hydrocarbon fragment. Auger electron spectra recorded after temperature-programmed reaction of ethylene sulfide reveal that approximately 15% of irreversibly chemisorbed ethylene sulfide decomposes to surface carbon, surface sulfur, and gaseous dihydrogen.

Preadsorbed hydrogen does not affect the yield of either ethylene peak nor does preadsorbed hydrogen result in formation of any new products such as ethane. Reaction of ethylene sulfide on a surface presaturated with deuterium reveals no deuterium incorporation into either the ethylene produced upon adsorption or that which evolves at 220 K, confirming that ethylene elimination is wholly intramolecular. Although deuterium-containing products (HD and D_2) are evident in all regions of the dihydrogen temperature programmed reaction spectrum, deuterium is preferentially incorporated into the 375 K peak.

These experiments further illustrate the dramatic effect of ring strain in determining the reaction selectivity of cyclic sulfides on Mo(110). Intramolecular elimination is the dominant reaction pathway for ethylene sulfide, with minor amounts (ca. 15%) of complete decomposition the only other detectable reaction. Importantly, these experiments also demonstrate that ring strain is not the sole determinant of reaction selectivity. No thiolate formation occurs despite the fact that ethylene sulfide is approximately as strained as trimethylene sulfide. The lack of thiolate formation may result from a more favorable entropy of activation for ethylene sulfide intramolecular elimination, an easily rationalized proposition if C–C bond formation is assumed to start early on the reaction coordinate(s) leading to intramolecular elimination. Ethylene sulfide and its derivatives are unique among cyclic sulfides because the carbons undergoing C–C bond formation during intramolecular elimination are already bonded to each other. Hence ethylene sulfide requres less structural reorganization (and activation entropy) for formation of the intramolecular elimination transition state(s). The size of the ethylene sulfide ring may therefore play a key role in the determination of its reaction selectivity.

Acknowledgment. This work was supported by the Department of Energy, Basic Energy Sciences, Grant no. DE-FG02-84ER13289.

(7) For a description of the apparatus used for this work see ref 1a. Ethylene sulfide was obtained from Aldrich and purified by distillation. Ethylene sulfide was degassed before use each day.

Gas-Phase Coupling of Methyl Radicals during the Catalytic Partial Oxidation of Methane

Kenneth D. Campbell, Edrick Morales, and Jack H. Lunsford*

Department of Chemistry, Texas A&M University College Station, Texas 77843

Received June 11, 1987

It is generally accepted that the initial step in the catalytic oxidative coupling of methane involves the homolytic cleavage of a C–H bond. This results in the formation of surface OH species and $CH_3^\bullet$ radicals which may undergo coupling to form ethane. A question arises as to whether the methyl radical coupling occurs on the surface or in the gas phase. Keller and Bhasin[1] proposed a mechanism for the catalytic oxidative coupling of CH_4 in which the formation of C_2H_6 resulted from the surface coupling of adsorbed $CH_3^\bullet$ radicals. In contrast to this mechanism, Lunsford and co-workers[2,3] proposed that a homogeneous gas-phase coupling of $CH_3^\bullet$ radicals, formed by the surface abstraction of H-atoms from CH_4, was the primary pathway for C_2H_6 formation. Evidence for the existence of gas-phase $CH_3^\bullet$ radicals during the oxidative coupling of CH_4 has been obtained by Driscoll et al.[3] with use of a matrix isolation electron spin resonance (MIESR) technique and, more recently, by Jones et al.[4] with use of the Paneth lead mirror technique.[5] The modeling studies of Labinger and Ott[6] and of Kimble and Kolts[7] also support the role of gas-phase $CH_3^\bullet$ radicals; however, the actual significance of these radicals in the formation of C_2H_6 has not been experimentally proven. In this communication a lower limit for the rate of gas-phase $CH_3^\bullet$ radical formation over a lithium-promoted MgO catalyst has been determined and this result is compared with the overall rate of C_2H_6 formation.

The experiments were carried out by using a modification of the MIESR apparatus[8] which is designed to detect gas-phase radicals emanating from surfaces of catalytic interest. In this system reactant gases along with argon are passed over a heated catalyst bed, and the effluent gases pass through a leak into a

(1) Keller, G. E.; Bhasin, M. M. *J. Catal.* **1982**, *73*, 9–19.
(2) Ito, T.; Wang, J. X.; Lin, C. H.; Lunsford, J. H. *J. Am. Chem. Soc.* **1985**, *107*, 5062–5068.
(3) Driscoll, D. J.; Martir, W.; Wang, J. X.; Lunsford, J. H.; *J. Am. Chem. Soc.* **1985**, *107*, 58–63.
(4) Jones, C. A.; Leonard, J. J.; Sofranko, J. A. *J. Catal.* **1987**, *103*, 311–319.
(5) Paneth, F.; Hofeditz, W. *Ber. Dtsch. Chem. Ges.* **1929**, *B62*, 1335.
(6) Labinger, J. A.; Ott, K. C. *J. Phys. Chem.* **1987**, *97*, 2682.
(7) Kimble, J. B.; Kolts, J. H. *Energy Progr.* **1986**, *6*, 226.
(8) Martir, W.; Lunsford, J. H. *J. Am. Chem. Soc.* **1981**, *103*, 3728–3732.

0002-7863/87/1509-7900$01.50/0

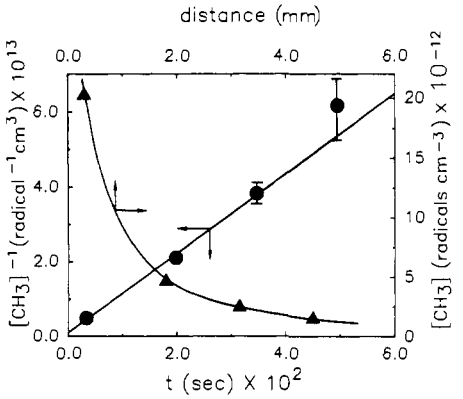

Figure 1. Plots of $[CH_3^{\bullet}]$ versus probe distance and $[CH_3^{\bullet}]^{-1}$ versus time (time for gas flow from catalyst bed to the probe).

Table I. Comparison of Gas-Phase Methyl Radicals and Ethane Production[a]

CH_4 molecules reacted (min^{-1})	1.4×10^{18}
CH_4 molecules to C_2's (min^{-1})	8.0×10^{17}
$CH_3^{\bullet}$ radicals exiting catalyst bed (min^{-1})[b]	3.2×10^{17}
$(CH_3^{\bullet}$ radicals$)/(CH_4$ reacted)	0.23
$(CH_3^{\bullet}$ radicals$)/(CH_4$ to C_2's)	0.40

[a] Reaction conditions: catalyst = 0.03 g of 7 wt% Li/MgO mixed with inert powdered quartz and supported in a thin layer of quartz wool. Temperature = 670 °C; atmospheric pressure; total flow = 880 cm^3 min^{-1} (STP); $Ar/CH_4/O_2$ = 219/9.3/1. [b] Radicals min^{-1} were detected, the collection efficiency in the sensitive region of the sapphire rod was 10%, and the percentage of molecules entering the leak was 0.28%.

low-pressure region where they are frozen on a sapphire rod maintained at 14 K. The sapphire rod with the matrix is then lowered into an ESR cavity where the spectrum is recorded. The original apparatus was converted into an atmospheric flow system through the construction of pressure leaks which allowed for the collection of ~2 cm^3 min^{-1} (STP) from the atmospheric stream. Moreover, the distance from the catalyst bed to the leak was adjustable. With this modification the gas-phase $CH_3^{\bullet}$ radical concentration at varying distances from the exit of the catalyst bed could be measured under atmospheric conditions. The radical collection efficiency was determined by carrying out a MIESR experiment with the stable NO_2 free radical.

Plots of $[CH_3^{\bullet}]$ versus distance and $[CH_3^{\bullet}]^{-1}$ versus time (time for gas flow from the catalyst bed to the probe) are shown in Figure 1. The slope of the $[CH_3^{\bullet}]^{-1}$ versus time plot should be the second-order rate constant for gas-phase $CH_3^{\bullet}$ radical coupling, and the intercept gives the gas-phase $CH_3^{\bullet}$ concentration at the exit of the catalyst bed. Analysis of the product stream was carried out with the use of standard GC techniques. From these results a direct comparison between the amounts of $CH_3^{\bullet}$ radicals and C_2 products was possible.

In establishing the slope of Figure 1 more weight was given to the greater concentrations obtained at short distances from the catalyst bed as these data were obtained at a much higher signal-to-noise ratio. A second-order rate constant for $CH_3^{\bullet}{}_{(g)}$ coupling of 1.1×10^{-11} cm^3 $radical^{-1}$ s^{-1} at 670 °C compares favorably with a "best value" of $(2.6 \pm 1) \times 10^{-11}$ cm^3 $radical^{-1}$ s^{-1} reported in a review by Warnatz.[9] The comparison of gas-phase $CH_3^{\bullet}$ radicals and C_2H_6 production is summarized in Table I. The results show that at least 40% of the C_2H_6 produced can be accounted for by the coupling of gas-phase $CH_3^{\bullet}$ radicals. Additional experiments to substantiate this result were carried out by placing the leak directly in contact with the catalyst bed. These experiments showed that >45% of the C_2H_6 could be accounted for by the gas-phase $CH_3^{\bullet}$ radicals.

In view of the tortuous path that the radicals must follow in leaving the polycrystalline catalyst particles and the catalyst bed it is expected that considerable recombination would occur before the radicals reach the exterior region of the bed. Thus, the value of 40–45% is a lower limit on the gas-phase reaction. Also, because of the nature of the bed, it is unlikely that the gas–surface equilibrium would have been perturbed to the point where surface recombination reactions would have been negated.

(9) Warnatz, J. In *Combustion Chemistry*; Gardiner, W. C., Ed.; Springer-Verlag: New York, 1984; pp 197–360.

Table II. Experimental and Simple Collision Theory Rates for C_2H_6 Formation[a]

	conc $CH_{3(g)}$,[b] radical cm^{-3}	conc $CH_{3(s)}$,[c] radical cm^{-2}	rate C_2H_6 prod., s^{-1}
gas phase	1.1×10^{14}		2.5×10^{15}[d]
surface coupling	1.1×10^{14}	8.8×10^{7}	1.5×10^{15}[e]
Rideal–Eley	1.1×10^{14}	8.8×10^{7}	6.6×10^{13}[e]

[a] Calculations are for T = 670 °C. [b] Concentration is the value at the exit of the catalyst bed. [c] Value assumes that the virtual pressure at the surface is 20 times that of the gas phase. [d] Value obtained from Table I assumes all gas-phase radicals couple. [e] Results obtained by using a reaction efficiency of 0.06. This value was determined by comparing the coupling rate to the collision frequency.

It was of interest to compare the experimental results with results predicted from simple collision theory for the surface coupling of adsorbed $CH_3^{\bullet}$ radicals and also for C_2H_6 formation according to a Rideal–Eley mechanism; i.e., a gas-phase $CH_3^{\bullet}$ radical reacting with a surface radical. These results are summarized in Table II. The results indicate that a Rideal–Eley mechanism is probably not important for this process. As a result of the assumptions used the experimental gas-phase and surface-coupling rates are comparable; however, it should be realized that the surface coupling calculation assumes a two-dimensional perfect gas velocity to describe the mobility of the adsorbed $CH_3^{\bullet}$ radicals. The latter assumption ignores the fact that an adsorption process which would result in a high virtual pressure would also limit the mobility of the radicals across the surface.

In conclusion, the results presented here show that gas-phase coupling of methyl radicals during the catalytic oxidative coupling of CH_4 represents a major mechanistic pathway for the formation of C_2H_6.

Acknowledgment. This research was supported by the Division of Basic Energy Sciences, Department of Energy.

Expeditious Enantioselective Syntheses of Indole Alkaloids of *Aspidosperma*- and *Hunteria*-Type

Manabu Node, Hideko Nagasawa, and Kaoru Fuji*

Institute for Chemical Research
Kyoto University, Uji, Kyoto 611, Japan

Received August 4, 1987

Indole alkaloids are known to possess a variety of physiological activities. The interest in *Aspidosperma* and *Hunteria* alkaloids is reflected in the numerous reports of syntheses of these alkaloids in the racemic and optically active forms.[1] The indole-2,3-quinodimethane strategy developed by Magnus[2] is among the most elegant racemic syntheses from the chemical point of view. The Pictet–Spengler or the Bischler–Napieralski condensation of tryptamine with the C_9 or C_{10} unit is the most widely accepted strategy because of the general applicability.[3] Here we describe

(1) (a) *Aspidosperma* alkaloids: Cordell, G. A. In *The Alkaloids*; Manske, R. H. F., Rodrigo, R. G. A., Eds.; Academic Press: New York, 1979; Vol. XVII, p 199. (b) *Hunteria* alkaloids: Döpke, W. In *The Alkaloid*; Manske, R. H. F., Rodrigo, R. G. A., Eds.; Academic Press: New York, 1981; Vol. XX, p 297. Atta-ur-Rahman; Sultana, M. *Heterocycles* **1984**, *22*, 841.

(2) (a) Magnus, P.; Gallagher, T.; Brown, P.; Pappalardo, P. *Acc. Chem Res.* **1984**, *17*, 35. (b) Magnus, P.; Pappalardo, P.; Southwell, I. *Tetrahedron* **1986**, *42*, 3215. (c) Magnus, P.; Pappalardo, P. *J. Am. Chem. Soc.* **1986**, *108*, 212 and references cited therein.

(3) Kutney, J. P. In *The Total Synthesis of Natural Products*; ApSimon, J., Ed.; John-Wiley & Sons: New York, 1979; Vol. 3, p 273.

0002-7863/87/1509-7901$01.50/0